

MICROLENSING DISCOVERY OF A POPULATION OF VERY TIGHT, VERY LOW-MASS BINARY BROWN DWARFS

J.-Y. CHOI¹, C. HAN^{1,101,112}, A. UDALSKI^{2,102}, T. SUMI^{3,103}, B. S. GAUDI^{4,101}, A. GOULD^{4,101}, D. P. BENNETT^{5,103}, M. DOMINIK^{6,104,105,111}, J.-P. BEAULIEU^{7,106}, Y. TSAPRAS^{8,9,105}, V. BOZZA^{10,11,104},

AND

F. ABE¹², I. A. BOND¹³, C. S. BOTZLER¹⁴, P. CHOTE¹⁵, M. FREEMAN¹⁴, A. FUKUI¹⁶, K. FURUSAWA¹², Y. ITOW¹², C. H. LING¹³, K. MASUDA¹², Y. MATSUBARA¹², N. MIYAKE¹², Y. MURAKI¹², K. OHNISHI¹⁷, N. J. RATTENBURY¹⁴, TO. SAITO¹⁸, D. J. SULLIVAN¹⁵, K. SUZUKI¹², W. L. SWEATMAN¹³, D. SUZUKI³, S. TAKINO¹², P. J. TRISTRAM¹⁹, K. WADA³, P. C. M. YOCK¹⁴

(THE MOA COLLABORATION),

M. K. SZYMAŃSKI², M. KUBIAK², G. PIETRZYŃSKI^{2,20}, I. SOSZYŃSKI², J. SKOWRON⁴, S. KOZŁOWSKI², R. POLESKI², K. ULACZYK², Ł. WYRZYKOWSKI^{2,21}, P. PIETRUKOWICZ²

(THE OGLE COLLABORATION)

L. A. ALMEIDA²², D. L. DEPOY²³, SUBO DONG²⁴, E. GORBIKOV²⁵, F. JABLONSKI²², C. B. HENDERSON⁴, K.-H. HWANG¹, J. JANCZAK²⁶, Y.-K. JUNG¹, S. KASPI²⁵, C.-U. LEE²⁷, U. MALAMUD²⁵, D. MAOZ²⁵, D. MCGREGOR⁴, J. A. MUÑOZ²⁸, B.-G. PARK²⁷, H. PARK¹, R. W. POGGE⁴, Y. SHVARTZVALD²⁵, I.-G. SHIN¹, J. C. YEE⁴

(THE μ FUN COLLABORATION)

K. A. ALSUBAI²⁹, P. BROWNE⁶, M. J. BURGDOFF³⁰, S. CALCHI NOVATI³¹, P. DODDS⁶, X.-S. FANG³², F. FINET³³, M. GLITRUP³⁴, F. GRUNDAHL³⁴, S.-H. GU³², S. HARDIS³⁵, K. HARPSØE^{35,36}, T. C. HINSE^{27,35}, A. HORNSTRUP³⁷, M. HUNDERTMARK^{6,38}, J. JESSEN-HANSEN^{34,39}, U. G. JØRGENSEN^{35,36}, N. KAINS^{6,40}, E. KERINS⁴¹, C. LIEBIG^{6,42}, M. N. LUND³⁴, M. LUNDKVIST³⁴, G. MAIER⁴², L. MANCINI^{11,43}, M. MATHIASSEN³⁵, M. T. PENNY^{4,41}, S. RAHVAR^{44,45}, D. RICCI^{33,46}, G. SCARPETTA^{10,31}, J. SKOTTFELT³⁵, C. SNODGRASS^{47,48}, J. SOUTHWORTH⁴⁹, J. SURDEJ³³, J. TREGLOAN-REED⁴⁹, J. WAMBSGANSS⁴², O. WERTZ³³, F. ZIMMER⁴²

(THE MINDSTEP CONSORTIUM)

M. D. ALBROW⁵⁰, E. BACHELET⁵¹, V. BATISTA⁴, S. BRILLANT⁴⁸, A. CASSAN⁵², A. A. COLE⁵³, C. COUTURES⁵², S. DIETERS⁵³, D. DOMINIS PRESTER⁵⁴, J. DONATOWICZ⁵⁵, P. FOUQUÉ⁵¹, J. GREENHILL⁵³, D. KUBAS^{48,52}, J.-B. MARQUETTE⁵², J. W. MENZIES⁵⁶, K. C. SAHU⁵⁷, M. ZUB⁴²

(THE PLANET COLLABORATION)

D. M. BRAMICH⁵⁸, K. HORNE⁶, I. A. STEELE⁵⁹, R. A. STREET⁸

(THE ROBO NET COLLABORATION)

¹Department of Physics, Institute for Astrophysics, Chungbuk National University, Cheongju 371-763, Republic of Korea

²Warsaw University Observatory, Al. Ujazdowskie 4, 00-478 Warszawa, Poland

³Department of Earth and Space Science, Osaka University, Osaka 560-0043, Japan

⁴Department of Astronomy, Ohio State University, 140 West 18th Avenue, Columbus, OH 43210, USA

⁵University of Notre Dame, Department of Physics, 225 Nieuwland Science Hall, Notre Dame, IN 46556-5670, USA

⁶SUPA, School of Physics & Astronomy, University of St Andrews, North Haugh, St Andrews KY16 9SS, UK

⁷Institut d'Astrophysique de Paris, UMR7095 CNRS–Université Pierre & Marie Curie, 98 bis boulevard Arago, F-75014 Paris, France

⁸Las Cumbres Observatory Global Telescope Network, 6740B Cortona Dr, Goleta, CA 93117, USA

⁹School of Physics and Astronomy, Queen Mary University of London, Mile End Road, London E1 4NS, UK

¹⁰INFN, Sezione di Napoli, Italy

¹¹Dipartimento di Fisica e E.R. Caianiello, Università di Salerno, Via Ponte Don Melillo 84084 Fisciano (SA), Italy

¹²Solar-Terrestrial Environment Laboratory, Nagoya University, Nagoya, 464-8601, Japan

¹³Institute of Information and Mathematical Sciences, Massey University, Private Bag 102-904, North Shore Mail Centre, Auckland, New Zealand

¹⁴Department of Physics, University of Auckland, Private Bag 92-019, Auckland 1001, New Zealand

¹⁵School of Chemical and Physical Sciences, Victoria University, Wellington, New Zealand

¹⁶Okayama Astrophysical Observatory, National Astronomical Observatory of Japan, Asakuchi, Okayama 719-0232, Japan

¹⁷Nagano National College of Technology, Nagano 381-8550, Japan

¹⁸Tokyo Metropolitan College of Aeronautics, Tokyo 116-8523, Japan

¹⁹Mt. John University Observatory, P.O. Box 56, Lake Tekapo 8770, New Zealand

²⁰Universidad de Concepción, Departamento de Astronomía, Casilla 160-C, Concepción, Chile

²¹Institute of Astronomy, University of Cambridge, Madingley Road, Cambridge CB3 0HA, UK

²²Instituto Nacional de Pesquisas Espaciais, São José dos Campos, SP, Brazil

²³Department of Physics, Texas A&M University, College Station, TX 77843, USA

²⁴Institute for Advanced Study, Einstein Drive, Princeton, NJ 08540, USA

²⁵School of Physics and Astronomy and Wise Observatory, Tel-Aviv University, Tel-Aviv 69978, Israel

²⁶Department of Physics, Ohio State University, 191 W. Woodruff, Columbus, OH 43210, USA

²⁷Korea Astronomy and Space Science Institute, Daejeon 305-348, Republic of Korea

²⁸Departamento de Astronomía y Astrofísica, Universidad de Valencia, E-46100 Burjassot, Valencia, Spain

²⁹Qatar Foundation, P.O. Box 5825, Doha, Qatar

³⁰HE Space Operations, Flughafenallee 24, 28199 Bremen, Germany

³¹Istituto Internazionale per gli Alti Studi Scientifici (IIASS), Vietri Sul Mare (SA), Italy

³²National Astronomical Observatories/Yunnan Observatory, Key Laboratory for the Structure and Evolution of Celestial Objects, Chinese Academy of Sciences, Kunming 650011, China

³³Institut d'Astrophysique et de Géophysique, Allé du 6 Août 17, Sart Tilman, Bât. B5c, 4000 Liège, Belgium

³⁴Stellar Astrophysics Center (SAC), Department of Physics and Astronomy, Aarhus University, Ny Munkegade 120, 8000 rhus C, Denmark

³⁵Niels Bohr Institute, University of Copenhagen, Juliane Maries vej 30, 2100 Copenhagen, Denmark

³⁶Centre for Star and Planet Formation, Geological Museum, Øster Voldgade 5, 1350 Copenhagen, Denmark

³⁷Institut for Rumforskning og-teknologi, Danmarks Tekniske Universitet, Juliane Maries Vej 30, 2100 København, Denmark

- ³⁸Institut für Astrophysik, Georg-August-Universität, Friedrich-Hund-Platz 1, 37077 Göttingen, Germany
³⁹Nordic Optical Telescope, Apartado 474, E-38700 Santa Cruz de La Palma, Spain
⁴⁰ESO Headquarters, Karl-Schwarzschild-Str. 2, 85748 Garching bei München, Germany
⁴¹Jodrell Bank Centre for Astrophysics, University of Manchester, Oxford Road, Manchester M13 9PL, UK
⁴²Astronomisches Rechen-Institut, Zentrum für Astronomie der Universität Heidelberg (ZAH), Mönchhofstr. 12-14, 69120 Heidelberg, Germany
⁴³Max Planck Institute for Astronomy, Königstuhl 17, 69117 Heidelberg, Germany
⁴⁴Department of Physics, Sharif University of Technology, P.O. Box 11155-9161, Tehran, Iran
⁴⁵Perimeter Institute for Theoretical Physics, 31 Caroline St. N., Waterloo, ON N2L2Y5, Canada
⁴⁶INAF/Istituto di Astrofisica Spaziale e Fisica Cosmica - Bologna, Via Gobetti 101, 40129 Bologna, Italy
⁴⁷Max Planck Institute for Solar System Research, Max-Planck-Str. 2, 37191 Katlenburg-Lindau, Germany
⁴⁸European Southern Observatory (ESO), Alonso de Cordova 3107, Casilla 19001, Santiago 19, Chile
⁴⁹Astrophysics Group, Keele University, Staffordshire ST5 5BG, UK
⁵⁰Department of Physics and Astronomy, University of Canterbury, Private Bag 4800, Christchurch 8020, New Zealand
⁵¹IRAP, Université de Toulouse, CNRS, 14 Avenue Edouard Belin, 31400 Toulouse, France
⁵²UPMC-CNRS, UMR 7095, Institut d'Astrophysique de Paris, 98bis boulevard Arago, F-75014 Paris, France
⁵³School of Mathematics and Physics, University of Tasmania, Private Bag 37, Hobart, TAS 7001, Australia
⁵⁴Department of Physics, University of Rijeka, Omladinska 14, 51000 Rijeka, Croatia
⁵⁵Department of Computing, Technical University of Vienna, Wiedner Hauptstrasse, Vienna, Austria
⁵⁶South African Astronomical Observatory, P.O. Box 9, Observatory 7925, South Africa
⁵⁷Space Telescope Science Institute, 3700 San Martin Drive, Baltimore, MD 21218, USA
⁵⁸European Southern Observatory, Karl-Schwarzschild-Str. 2, 85748 Garching bei München, Germany
⁵⁹Astrophysics Research Institute, Liverpool John Moores University, Liverpool CH41 1LD, UK
¹⁰¹The μ FUN Collaboration
¹⁰²The OGLE Collaboration
¹⁰³The MOA Collaboration
¹⁰⁴The MiNDSTeP Consortium
¹⁰⁵The RoboNet Collaboration
¹⁰⁶The PLANET Collaboration
¹¹¹Royal Society University Research Fellow and
¹¹²Corresponding author
Draft version August 6, 2018

ABSTRACT

Although many models have been proposed, the physical mechanisms responsible for the formation of low-mass brown dwarfs are poorly understood. The multiplicity properties and minimum mass of the brown-dwarf mass function provide critical empirical diagnostics of these mechanisms. We present the discovery via gravitational microlensing of two very low-mass, very tight binary systems. These binaries have directly and precisely measured total system masses of $0.025 M_{\odot}$ and $0.034 M_{\odot}$, and projected separations of 0.31 AU and 0.19 AU, making them the lowest-mass and tightest field brown-dwarf binaries known. The discovery of a population of such binaries indicates that brown dwarf binaries can robustly form at least down to masses of $\sim 0.02 M_{\odot}$. Future microlensing surveys will measure a mass-selected sample of brown-dwarf binary systems, which can then be directly compared to similar samples of stellar binaries.

Subject headings: gravitational lensing: micro – binaries: general

1. INTRODUCTION

Brown dwarfs (BD) are collapsed objects with masses below the minimum mass required to fuse hydrogen of $\sim 0.08 M_{\odot}$. Direct imaging surveys have found that isolated BD systems to be fairly ubiquitous in the field as well as in young clusters (see Luhman (2012) for a review), with frequencies rivaling those of their more massive hydrogen-fusing stellar brethren. However, it is unclear whether BDs simply represent the low-mass extension of the initial collapsed object mass function (IMF), and thus formed via the same processes as stars, or if their formation requires additional physical mechanisms.

The minimum mass of the IMF potentially provides an important discriminant between various models of BD formation, with very low mass BD binary systems being particularly important in this regard. This is because predictions for the multiplicity properties of low-mass BDs – frequency, mass ratio, and separation as a function of total system mass and age – differ significantly depending on the formation scenario. Nowever, the currently available observational samples are strongly influenced by detection biases and selection ef-

fects. For example, although BD surveys in young stellar associations allow for detections of low-mass BD systems, these associations are typically fairly distant, making it difficult to detect tight BD binaries. Conversely, field BD binaries can be resolved to much smaller separations, but low-mass, old field BDs are quite faint and thus difficult to detect. As a result, the current sample of binary BDs is not only small in number but is also substantially incomplete, particularly in the regime of low mass and small separation. A further complication is that direct mass measurements are available only for a subset of tight field BD binaries. Mass estimates of other systems must rely on comparison with models, resulting in substantial systematic uncertainties.

Gravitational microlensing is well-suited to fill the gap. Microlensing is the astronomical phenomenon wherein the brightness of a star is magnified by the bending of light caused by the gravity of an intervening object (lens) located between the background star (source) and an observer. Since this effect occurs regardless of the lens brightness, microlensing is suitable to detect faint objects such as BDs (Paczynski 1986). For a lensing event produced by a binary lens with well resolved brightness variation of the lensed star, it is possible to pre-

cisely measure the physical parameters of the lensing object including the mass and distance. Here we report the discovery and characterization of two binary BD systems, which both have very low mass and tight separation, thus constituting a new population.

2. OBSERVATION

These BD binaries were discovered in microlensing events OGLE-2009-BLG-151/MOA-2009-BLG-232 and OGLE-2011-BLG-0420. The events occurred on stars located in the Galactic Bulge field with equatorial and Galactic coordinates $(RA, DEC)_{2000} = (17^h54^m22.34^s, -29^\circ03'20.8'')$, $(l, b)_{2000} = (0.88^\circ, -1.70^\circ)$ and $(RA, DEC)_{2000} = (17^h50^m56.18^s, -29^\circ49'30.2'')$, $(l, b)_{2000} = (359.84^\circ, -1.45^\circ)$, respectively.

OGLE-2009-BLG-151/MOA-2009-BLG-232 was first discovered by the Optical Gravitational Lensing Experiment (OGLE: Udalski (2003)) group and was independently discovered by the Microlensing Observations in Astrophysics (MOA: Bond, et al. (2001); Sumi et al. (2003)) group in 2009 observation season. OGLE-2011-BLG-0420 was detected by the OGLE group in the 2011 season. Both events were additionally observed by follow-up observation groups including Microlensing Follow-Up Network (μ FUN: Gould et al. (2006)), Probing Lensing Anomalies Network (PLANET: Beaulieu et al. 2006), RoboNet (Tsapras et al. (2009)), and Microlensing Network for the Detection of Small Terrestrial Exoplanets (MiNDSTEP: Dominik et al. (2010)). In Table 1, we list the survey and follow-up groups along with their telescope characteristics. Data reductions were carried out using photometry codes developed by the individual groups.

3. ANALYSIS

Figure 1 displays the light curves of the individual events. OGLE-2009-BLG-151/MOA-2009-BLG-232 is characterized by two strong spikes flanking a “U”-shape trough, which is typical for caustic-crossing binary-lens events. Caustics denote positions on the source plane where the lensing magnification of a point source diverges (Petters et al. 2001). When a caustic is formed by an astronomical object composed of 2 masses, it forms a single or multiple sets of closed curves each consisting of concave curves that meet at cusps. When a source star crosses the caustic, its brightness is greatly enhanced, causing strong deviation from the smooth and symmetric single-lens light curve. The light curve of OGLE-2011-BLG-0420, on the other hand, appears to be smooth and symmetric, which are the characteristics of a lensing event caused by a single mass. From the fit based on the single lens model, however, the light curve exhibits noticeable deviations near the peak, which indicates the existence of a companion to the lens. According to the classification scheme of binary signatures in lensing light curves set by Ingrasso et al. (2009), the deviations of OGLE-2009-BLG-151/MOA-2009-BLG-232 and OGLE-2011-BLG-0420 are classified as Class II and I, respectively.

With known binary signatures, we conduct binary-lens modeling of the observed light curves. For a single lens, the light curve is described by 3 parameters: the time of closest lens-source approach, t_0 , the lens-source separation (normalized by the Einstein-ring radius, θ_E) at that time, u_0 , and the Einstein time scale, t_E , which represents the time required for the source to cross θ_E . The Einstein ring denotes the image of a source in the event of perfect lens-source alignment, and so is used as the length scale of lensing phenomena. Binary

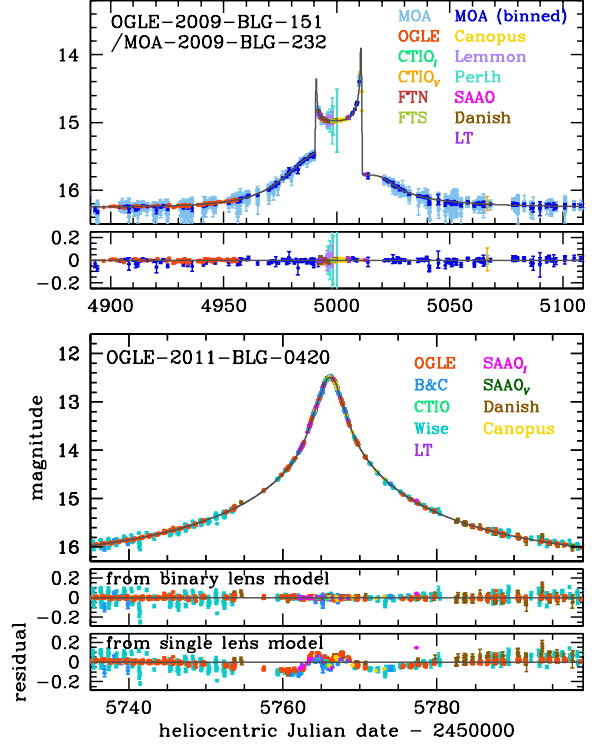


FIG. 1.— Light curves of the binary BD microlensing events OGLE-2009-BLG-151/MOA-2009-BLG-232 and OGLE-2011-BLG-0420. For the MOA data of OGLE-2009-BLG-151/MOA-2009-BLG-232, binned data are additionally plotted to better show residuals.

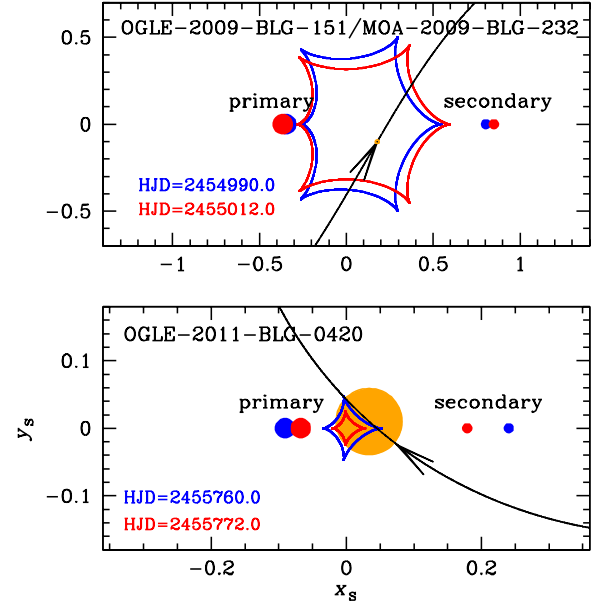


FIG. 2.— Geometry of the lens systems. In each panel, the cuspy closed figure represents the caustic, the small filled dots are the locations of the binary lens components, and the curve with an arrow represents the source trajectory. Two sets of lens positions and the corresponding caustics are presented at the times marked in the panel. The circle on the source trajectory represents the scale of the source star with respect to the caustic. All lengths are normalized by the Einstein radius corresponding to the total mass of the lens.

lenses require three additional parameters: the mass ratio, q ,

TABLE 1
TELESCOPES

event	telescope
OGLE-2009-BLG-151 /MOA-2009-BLG-232	MOA, 1.8m Mt. John, New Zealand OGLE, 1.3m Warsaw, Las Campanas, Chile μ FUN, 1.3m SMARTS, Cerro Tololo Inter-American (CTIO), Chile μ FUN, 1.0m Mt. Lemmon, USA PLANET, 1.0m Canopus, Australia PLANET, 1.0m South African Astronomical (SAAO), South Africa PLANET, 0.6m Perth, Australia MiNDSTeP, 1.54m Danish, La Silla, Chile RoboNet, 2.0m Faulkes North Telescope (FTN), Hawaii, USA RoboNet, 2.0m Faulkes South Telescope (FTS), Hawaii, USA RoboNet, 2.0m Liverpool Telescope (LT), Canary Islands, Spain
OGLE-2011-BLG-0420	OGLE, 1.3m Warsaw, Las Campanas, Chile MOA, 0.6m B&C, Mt. John, New Zealand μ FUN, 1.3m SMARTS, CTIO, Chile μ FUN, 1.0m Wise, Israel PLANET, 1.0m SAAO, South Africa PLANET, 1.0m Canopus, Australia MiNDSTeP, 1.54m Danish, La Silla, Chile RoboNet, 2.0m LT, Canary Islands, Spain

the projected separation (normalized by θ_E) between the binary components, s , and the angle between the source trajectory and the binary axis, α (source trajectory angle).

In addition to the basic lensing parameters, it is often needed to include additional parameters to precisely describe subtle light-curve features caused by various second-order effects. For both events, the lensing-induced magnification lasted for several months, which comprises a significant fraction of the Earth's orbital period around the Sun (1 year). Then, the apparent motion of the source with respect to the lens deviates from rectilinear (Gould 1992) due to the change of the observer's position caused by the Earth's orbital motion. This parallax effect causes long-term deviation in lensing light curves. Consideration of the parallax effect requires 2 additional parameters of $\pi_{E,N}$ and $\pi_{E,E}$, which are the two components of the lens parallax vector π_E , projected on the sky along the north and east equatorial coordinates, respectively. The orbital motion of the lens also affects lensing light curves. The lens orbital motion causes the projected binary separation and the source trajectory angle to change over the course of a lensing event. These require two additional lensing parameters of the change rates of the binary separation, ds/dt , and the source trajectory angle, $d\alpha/dt$. Finally, finite-source effects become important whenever the magnification varies very rapidly with the change of the source position, so that different parts of the source are magnified by different amounts. Such a rapid magnification variation occurs near caustics and thus finite-source effects are important for binary-lens events involved with caustic crossings or approaches. This requires one more parameter, the normalized source radius $\rho_* = \theta_*/\theta_E$, where θ_* is the angular source radius. Measuring the deviation caused by the parallax and finite-source effects is important to determine the physical parameters of the lens. By measuring the finite-source effect, the Einstein radius is determined by $\theta_E = \theta_*/\rho_*$ once the source radius is known. With the measured lens parallax and the Einstein radius, the mass and distance to the lens are determined as $M_{\text{tot}} = \theta_E/(\kappa\pi_E)$ and $D_L = \text{AU}/(\pi_E\theta_E + \pi_S)$, respectively (Gould 1992; Gould et al. 2006). Here $\kappa = 4G/(c^2\text{AU})$, AU is an Astronomical Unit, $\pi_S = \text{AU}/D_S$, and $D_S \sim 8$ kiloparsec is the source distance.

We model the observed light curves by minimizing χ^2 in the

TABLE 2
BEST FIT LENSING PARAMETERS

parameters	OGLE-2009-BLG-151 /MOA-2009-BLG-232	OGLE-2011-BLG-0420
χ^2/dof	3040.9/3032	5410.3/5439
t_0 (HJD')	4999.680 ± 0.061	5766.110 ± 0.001
u_0	-0.217 ± 0.004	-0.030 ± 0.001
t_E (days)	27.95 ± 0.11	35.22 ± 0.08
s	1.135 ± 0.004	0.289 ± 0.002
q	0.419 ± 0.006	0.377 ± 0.009
α	-1.049 ± 0.004	-2.383 ± 0.002
ρ_* (10^{-2})	1.06 ± 0.01	4.88 ± 0.01
$\pi_{E,N}$	-3.33 ± 0.11	-1.15 ± 0.05
$\pi_{E,E}$	-0.91 ± 0.11	0.19 ± 0.01
ds/dt (yr^{-1})	1.55 ± 0.13	-2.59 ± 0.07
$d\alpha/dt$ (yr^{-1})	0.69 ± 0.06	6.88 ± 0.20
slope (mag yr^{-1})	0.0052 ± 0.0008	—

NOTE. — HJD' = HJD - 2450000.

parameter space. We investigate the existence of possible degenerate solutions because it is known that light curves resulting from different combinations of lensing parameters often result in a similar shape (Griest & Safazadeh 1998; Dominik 1999; An 2005). In modeling finite-source effects, we additionally consider the limb-darkening variation of the source star surface (Witt 1995) by modeling the surface profile as a standard linear law. For χ^2 minimization, we use the Markov Chain Monte Carlo method. Photometric errors of the individual data sets are rescaled so that χ^2 per degree of freedom becomes unity for each data set. We eliminate data points with large errors and those lying beyond 3σ from the best-fit model to minimize their effect on modeling.

Table 2 gives the solutions of the lensing parameters found from modeling. In Figure 2, we also present the geometry of the lens system where the source trajectory with respect to the positions of the binary lens components and the caustic are shown. For OGLE-2009-BLG-151/MOA-2009-BLG-232, we find that the two strong spikes were produced by the source crossings of a big caustic formed by a binary lens with the projected separation between the lens components ($s \sim 1.14$) being similar to the Einstein radius of the lens. We find that including the second-order effects of lens parallax and orbital motions improves the fit by $\Delta\chi^2 = 213$. OGLE-

TABLE 3
SOURCE STAR PROPERTIES

quantity	OGLE-2009-BLG-151 /MOA-2009-BLG-232	OGLE-2011-BLG-0420
$(V-I)_0$	1.352	1.611
I_0	14.490	13.091
θ_* (μ as)	7.57 ± 0.66	15.94 ± 1.38
stellar type	K giant	K giant
θ_E (mas)	0.71 ± 0.01	0.33 ± 0.03

2011-BLG-0420 is also a caustic-crossing event, but the projected binary separation ($s \sim 0.29$) is substantially smaller than the Einstein radius. For such a close binary lens, the caustic is small. For OGLE-2011-BLG-0420, the caustic is so small that the source size is similar to that of the caustic. Hence, the lensing magnification is greatly attenuated by the severe finite-source effect and thus the deviation during the caustic crossings is weak. We find that there exists an alternative solution with $s > 1$ caused by the well-known close/wide binary degeneracy, but the degeneracy is resolved with $\Delta\chi^2 = 27$. The parallax and lens orbital effects are also clearly measured with $\Delta\chi^2 = 403$. From 10 years of OGLE data, we find that OGLE-2011-BLG-0420S (source star) is extremely stable, but OGLE-2009-BLG-151/MOA-2009-BLG-232S exhibits irregular $< 1\%$ variations, typically on time scales of a few hundred days. Because these can affect the parallax measurement, we restrict the modeling to $t_0 \pm 300$ days to minimize the impact of variations while still retaining enough baseline to ensure a stable fit. We also include a "slope" parameter for the source flux to account for the remaining variability. We find only slight differences in final results if we repeat this procedure with longer baselines. Therefore, it is unlikely but not impossible that source variability affects the OGLE-2009-BLG-151/MOA-2009-BLG-232 parallax measurement. By contrast, the results for OGLE-2011-BLG-0420 are very robust.

4. PHYSICAL PARAMETERS

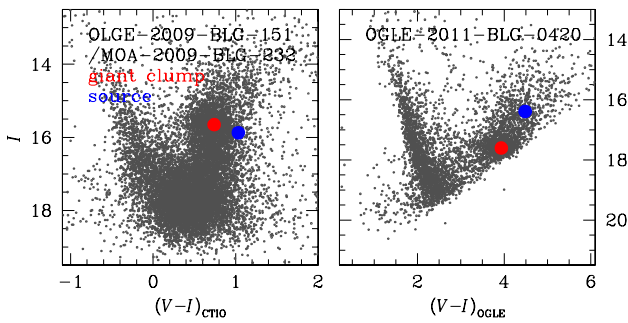


FIG. 3. — Locations of the lensed stars of the individual events on the color-magnitude diagrams.

Since ρ_* and π_E are well measured (Table 2), it is possible to determine M_{tot} and D_L for both systems. The only missing ingredient is the angular source radius θ_* , needed to find $\theta_E = \theta_*/\rho_*$. This is determined from the de-reddened color and brightness of the source star. For the calibration of the color and brightness, we use the centroid of bulge giant clump as a reference (Yoo et al. 2004) because its de-reddened brightness $I_{0,c} = 14.45$ at the Galactocentric distance (Nataf et al. 2012) and the color $(V-I)_{0,c} = 1.06$ (Bensby et al.

TABLE 4
PHYSICAL QUANTITIES

quantity	OGLE-2009-BLG-151 /MOA-2009-BLG-232	OGLE-2011-BLG-0420
$M_{\text{tot}} (M_\odot)$	0.025 ± 0.001	0.034 ± 0.002
$M_1 (M_\odot)$	0.018 ± 0.001	0.025 ± 0.001
$M_2 (M_\odot)$	0.0075 ± 0.0003	0.0094 ± 0.0005
D_L (kpc)	0.39 ± 0.01	1.99 ± 0.08
d_\perp (AU)	0.31 ± 0.01	0.19 ± 0.01

2011) are known. We then translate $V-I$ into $V-K$ color by using the relation (Bessell & Brett 1988) and then find θ_* using the relation between the $V-K$ and the angular radius (Kervella et al. 2004). In Table 3, we list the measured de-reddened colors $(V-I)_0$, magnitudes I_0 , angular radii, types of the source stars and the measured Einstein radii of the individual events. Figure 3 shows the locations of the lensed stars of the individual events on the color-magnitude diagrams.

The derived physical quantities for the OGLE-2009-BLG-151/MOA-2009-BLG-232L and OGLE-2011-BLG-0420L binaries are listed in Table 4. Here the letter "L" at the end of each event indicates the lens of the event. The total system masses are $M_{\text{tot}} = (0.025 \pm 0.001) M_\odot$ and $(0.034 \pm 0.002) M_\odot$, respectively, well below the hydrogen-burning limit. The projected separations and mass ratios are $d_\perp = (0.31 \pm 0.01)$ AU and $q = 0.419 \pm 0.006$ for OGLE-2009-BLG-151/MOA-2009-BLG-232L, and $d_\perp = (0.19 \pm 0.01)$ AU and $q = 0.377 \pm 0.009$ for OGLE-2011-BLG-0420L. It is worth emphasizing the high precisions ($< 10\%$) with which the total system masses and individual component masses are determined.

Figure 4 compares OGLE-2009-BLG-151/MOA-2009-BLG-232L and OGLE-2011-BLG-0420L to a sample of low-mass binaries in the field and in young associations from Faherty et al. (2011), Basri & Martín (1999), Burgasser et al. (2008), Burgasser et al. (2012), and Lane et al. (2001). The only known BD binaries with comparable total masses are Oph 16225-240515 with $M_{\text{tot}} \sim 0.032 M_\odot$ (Jayawardhana & Ivanov 2006) and 2MASSJ1207334-393254 (Chauvin et al. 2004) with $M_{\text{tot}} \sim 0.028 M_\odot$. However, these two systems are both young (5 Myr and 8 Myr, respectively), and have very wide separations of hundreds of AU. Indeed, OGLE-2009-BLG-151/MOA-2009-BLG-232L and OGLE-2011-BLG-0420L are the tightest known BD binaries with substantially lower mass than previously known field BD binaries. Both systems have mass ratios of ~ 0.4 , apparently consistent with the trend found from old field BDs, which tend to have a preference for larger mass ratios (see Figure 3 of Burgasser et al. (2007)), although it is important to stress that the selection effects in microlensing and direct imaging surveys are very different.

Burgasser et al. (2007) suggested that field low-mass binaries with $M_{\text{tot}} = 0.05 - 0.2 M_\odot$ may exhibit an empirical lower limit to their binding energies of $Gm_1m_2/a \sim 2.5 \times 10^{42}$ erg (see Figure 5). Although OGLE-2009-BLG-151/MOA-2009-BLG-232L and OGLE-2011-BLG-0420L are substantially lower in mass than these BD binaries, they are also considerably tighter. Therefore, with binding energies of $\sim 7 \times 10^{42}$ erg and 2×10^{43} erg, they are consistent with the extrapolation of the minimum binding energy limit down to total system masses of $M_{\text{tot}} \sim 0.02 M_\odot$.

Although we are unable to provide an estimate of the space density of such tight, low-mass brown dwarf binaries, nor

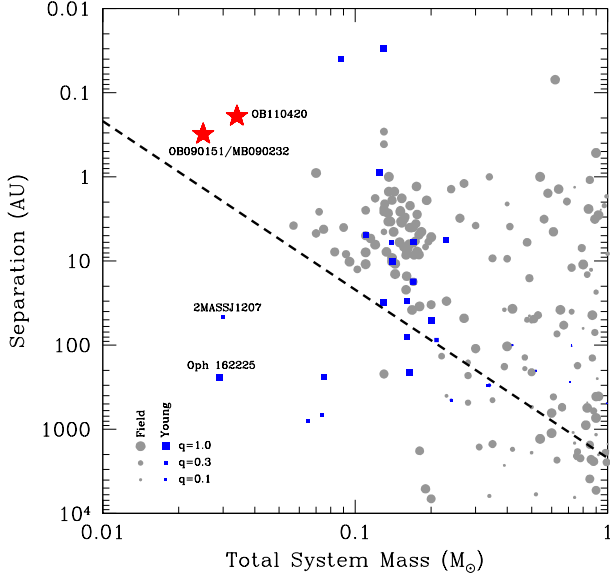


FIG. 4.— Projected separation versus total system mass for a compilation of binaries. Grey circles indicate old field binaries, whereas blue squares indicate young (< 500 Myr) systems. The size of the symbols is proportional to the square root of the mass ratio. The red stars are the two tight, low-mass binary BDs discussed here, which have mass ratios of ~ 0.4 . The dashed line shows a binding energy of 2×10^{42} erg, assuming a mass ratio of 1.

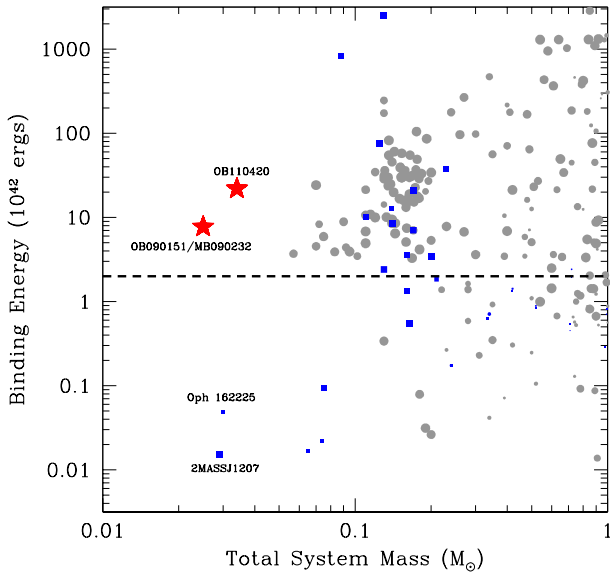


FIG. 5.— Binding energy (Gm_1m_2/a) versus total system mass for the same binaries as shown in Fig. 4. Symbols and line are the same.

even an estimate of their frequency relative to more massive stellar binaries, the discovery of two systems among the relatively small sample of binary lensing events with precise mass estimates strongly suggests that very low-mass, very tight BD binaries are not rare. Thus these detections herald a much larger population of such systems. We can therefore conclude that BD binaries can robustly form at least down to system masses of $\sim 0.02 M_\odot$, providing a strong constraint for formation models.

5. DISCUSSION

The discoveries of the binary BDs reported in this paper demonstrate the importance of microlensing in BD studies. The microlensing method has various advantages. First, it enables to detect faint old populations of BDs that could not be studied by the conventional method of imaging surveys and the sensitivity extends down to planetary mass objects (Sumi et al. 2011). It also allows one to detect BDs distributed throughout the Galaxy. Therefore, microlensing enables to study BDs based on a sample that is not biased by the brightness and distance. Second, in many cases of microlensing BDs, it is possible to precisely measure the mass, which is not only the most fundamental physical parameter but also a quantity enabling to unambiguously distinguish BDs from other low mass populations such as low mass stars. While mass measurements by the conventional method require long-term and multiple stage observation of imaging, astrometry, and spectroscopy by using space-borne or very large ground-based telescopes, microlensing requires simple photometry by using 1 m class telescopes. Despite the observational simplicity, the mass can be measured with uncertainties equivalent to or smaller than those of the measurement by conventional methods. Finally, microlensing can expand the ranges of masses and separations in the binary BD sample that is incomplete below $\sim 0.1 M_\odot$ in mass and ~ 3 AU in separation. Microlensing sensitivity to binary objects peaks when the separation is of order the Einstein radius. Considering that the Einstein radius corresponding to a typical binary BD is < 1 AU, microlensing method will make it possible to study binary BDs with small separations.

The number of microlensing BDs is expected to increase in the future with the upgrade of instruments in the existing survey experiments and the advent of new surveys. The OGLE group recently upgraded its camera with a wider field of view to significantly increase the observational cadence. The Korea Microlensing Telescope Network (KMTNet), now being constructed, will achieve 10 minute sampling of all lensing events by using a network of 1.6 m telescopes on three different continents in the Southern hemisphere with wide-field cameras. Furthermore, there are planned lensing surveys in space including EUCLID and WFIRST. With the increase of the microlensing event rate combined with the improved precision of observation, microlensing will become a major method to study BDs.

Work by C.Han was supported by the research grant of Chungbuk National University in 2011. The OGLE project has received funding from the European Research Council under the European Community's Seventh Framework Programme (FP7/2007-2013) / ERC grant agreement no. 246678. The MOA experiment was supported by grants JSPS22403003 and JSPS23340064. This work is based in part on data collected by MiNDSTeP with the Danish 1.54m telescope at the ESO La Silla Observatory, which is operated based on a grant from the Danish Natural Science Foundation (FNU). The MiNDSTeP monitoring campaign is powered by ARTEMIS (Dominik et al. 2008, AN 329, 248). MH acknowledges support by the German Research Foundation (DFG). DR (boursier FRIA), FF (boursier ARC) and JSurdej acknowledge support from the Communauté française de Belgique – Actions de recherche concertées – Académie universitaire Wallonie-Europe. KA, DMB, MD, KH, MH, CL, CS, RAS, and YT are thankful to Qatar National Research

Fund (QNRf), member of Qatar Foundation, for support by grant NPRP 09-476-1-078. CS has received funding from FP7/2007-2013 under grant agreement no. 268421. KH is supported by a Royal Society Leverhulme Trust Senior Research Fellowship. AG and BSG acknowledge support from NSF AST-1103471. BSG, AG, and RWP acknowledge support from NASA grant NNX12AB99G. Work by JCY is supported by a National Science Foundation Graduate Research

Fellowship under Grant No. 2009068160. SDongar's research was performed under contract with the California Institute of Technology funded by NASA through the Sagan Fellowship Program. TS was supported by the grant JSPS23340044. YM acknowledges support from JSPS grants JSPS23540339 and JSPS19340058. TCH and CUL acknowledge the support of KASI grant 2012-1-410-02 and KRCF.

REFERENCES

- An, J. H. 2005, *MNRAS*, 356, 1409
 Basri, G., & Martín, E. L. 1999, *AJ*, 118, 2460
 Beaulieu, J.-P., Bennett, D. P., Fouqué, P., et al., 2006, *Nature* 439, 437
 Bensby, T., Adén, D., Meléndez, J., et al., 2011, *A&A*, 533, 134
 Bessell, M. S., & Brett, J. M. 1988, *PASP*, 100, 1134
 Bond, I. A., Abe, F., Dodd, R. J., et al. 2001, *MNRAS*, 327, 868
 Burgasser, A. J., Reid, I. N., Siegler, N., et al. 2007, *Protostars and Planets*, eds. V. J. Reipurth, D. Jewitt, and K. Keil (Tucson, Univ. of Arizona Press), 427
 Burgasser, A. J., Liu, M. C., Ireland, M. J., Cruz, K. L., & Dupuy, T. J. 2008, *ApJ*, 681, 579
 Burgasser, A. J., Luk, C., Dhital, S., et al. 2012, *ApJ*, 757, 110
 Chauvin, G., Lagrange, A.-M., Dumas, C., et al. 2004, *A&A*, 425, L29
 Dominik, M. 1999, *A&A*, 349, 108
 Dominik, M., Horne, K., Allan, A., et al. 2008, *Astron. Nachr.*, 329, 248
 Dominik, M., Jørgensen, U. G., Rattenbury, N. J., et al. 2010, *Astron. Nachr.*, 331, 671
 Faherty, J. K., Burgasser, A. J., Bochanski, J. J., Looper, D. L., West, A. A., & van der Blik, N. S. 2011, *A&A*, 141, 71
 Gould, A. 1992, *ApJ*, 392, 442
 Gould, A., Udalski, A., An, D., et al., 2006, *ApJ*, 644, L37
 Griest, K., & Safazadeh, N. 1998, *ApJ*, 500, 37
 Ingrassio, G., Novati, S. C., de Paolis, F., et al. 2009, *MNRAS*, 399, 219
 Jayawardhana, R., & Ivanov, V. D. 2006, *Science*, 313, 1279
 Kervella, P., Thévenin, F., Di Folco, E., & Ségransan, D. 2004, *A&A*, 426, 297
 Lane, B. F., Zapatero Osorio, M. R., Britton, M. C., Martín, E. L., & Kulkarni, S. R. 2001, *ApJ*, 560, 390
 Luhman, K. L. 2012, *ARA&A*, 50, 65
 Nataf, D. M., Gould, A., Fouqué, P., et al., 2012, *arXiv1208.1263*
 Paczyński, B. 1986, *ApJ*, 304, 1
 Petters, A. O., Levine, H., Wambsganss, J. 2001, *Singularity Theory and Gravitational Lensing*, *Progress in Mathematical Physics*, v21 (Birkhäuser)
 Sumi, T., Abe, F., Bond, I. A., et al. 2003, *ApJ*, 591, 204
 Sumi, T., Kamiya, K., Bennett, D. P., et al. 2011, *Nature*, 473, 349
 Tsapras, Y., Street, R., Horne, K., et al., 2009, *Astron. Nachr.*, 330, 4
 Udalski, A. 2003, *Acta Astron.*, 53, 291
 Witt, H. J. 1995, *ApJ*, 449, 42
 Yoo, J., DePoy, D. L., Gal-Yam, A., et al. 2004, *ApJ*, 603, 139